A MPPT ALGORITHM FOR SINGLE-PHASE SINGLE-STAGE PHOTOVOLTAIC CONVERTERS

Gabriele Grandi, Claudio Rossi, Domenico Casadei

Dept. of Electrical Engineering
University of Bologna, ITALY

Abstract: A maximum power point tracking algorithm for single-stage converters connecting photovoltaic panels to a single-phase grid is presented in this paper. The algorithm is based on the processing of current and voltage low-frequency oscillations introduced in the PV panels by the single-phase utility grid. The algorithm has been developed to allow an array of PV modules to be connected to the grid by using a single-stage converter. This simple structure yields higher efficiency and reliability when compared with standard solutions based on double-stage converters configuration. The proposed maximum power point tracking algorithm has been numerically simulated and experimentally verified by means of a converter prototype connected to a single-phase grid.

Keywords: Converters, Solar energy, Renewable energy systems, Efficiency, Inverters.

1. INTRODUCTION

One of the most promising candidates for the large scale spreading of renewable energy source is the photovoltaic technology. In particular, photovoltaic roofs give an important share of new installations of PV panels. For these applications the rated power is lower than 5 kW and the PV panels are permanently connected to a single-phase grid. The power flow between the PV panels and the grid is controlled by a power conditioning system (PCS), which should be reliable and inexpensive. To obtain the maximum efficiency of the system, the PCS must keep the power extracted from the PV panels close to the maximum power point (MPP). Several solutions for PCS with maximum power point tracking (MPPT) capability have been recently proposed, based on both single-stage (Kuo *et al*., 2001) and double-stage converter topologies (Gow *et al*., 2000).

This paper deals with a single-phase, single-stage PCS configuration, using a simple and effective MPPT embedded algorithm. The scheme of the proposed system is shown in Fig. 1. The output of the PV panels is directly connected to the dc-link of the single-phase inverter (VSI type), and the output of the inverter is connected to the grid through the ac-link inductor L_{ac}.

2. OPERATING PRINCIPLE

The VSI output voltage v_F is controlled in order to force the current injected into the mains i_S to follow a sinusoidal reference waveform, synchronized and in phase with the fundamental component of the source voltage v_S. As a consequence, a sinusoidal current is obtained even in presence of voltage perturbations coming from the mains. The amplitude of the reference source current I_S^* is generated by the dc-link voltage regulator on the basis of the error between the dc-link voltage V_{dc} and the reference dc voltage V_{dc}^* of the PV panels.

The MPPT algorithm varies V_{dc}^* according to the environmental conditions in order to keep the operating point of the PV panels close to the MPP.

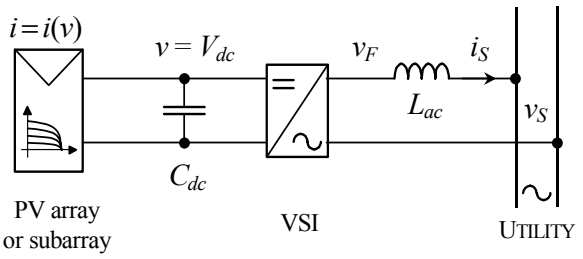

Fig. 1. Schematic diagram of the PV generation system

The basic principle of the MPPT algorithm is to exploit current and voltage oscillations caused by the double-frequency pulsations of the instantaneous power, which are inherent in single-phase power systems. Analyzing these oscillations it is possible to obtain information about the power gradient, evaluating if the PV system operates close to the maximum power point.

As it is known, for a non-null value of active power injected into a single-phase grid P_S, the instantaneous power $p_S(t)$ pulsates at a frequency twice than that of the grid. If the current $i_S(t)$ is in phase with the source voltage $v_S(t)$, the instantaneous value of power injected into the grid is

$$p_S(t) = v_S(t)\, i_S(t) = \sqrt{2}V_S \cos \omega t \sqrt{2} I_S \cos \omega t = V_S I_S (1 + \cos 2\omega t). \quad (1)$$

The average quantity $V_S I_S$ corresponds to the active power P_S. The power pulsation at the angular frequency 2ω in (1) is reflected on the dc-link bus of the VSI as a voltage pulsation superimposed to the dc-link voltage V_{dc}. The variation of V_{dc} can be related to active power P_S, grid angular frequency ω, and dc-link capacitor C_{dc} by the following relationship:

$$\frac{P_S}{\omega} = C_{dc}(V_{dcMAX}^2 - V_{dcMIN}^2) \cdot \quad (2)$$

The dc-link voltage excursion $(V_{dcMAX} - V_{dcMIN})$ can be limited by choosing a proper value for C_{dc}, according with (2), ensuring the correct operation of the inverter. The residual oscillation of V_{dc} determines a small pulsation of the power supplied by the PV panels. On the basis of the phase relationship between power and voltage oscillations, the MPPT algorithm moves the operating point of the PV panels by varying V_{dc}^* until the MPP is reached. Voltage and current oscillations must be as small as possible in order to minimize the oscillation of power extracted from the panel. On the other hand, these oscillations must be large enough to be sensed and distinguished from current and voltage ripple due to the VSI switching effects. It has been observed that keeping voltage and current oscillation around 1% of their rated values leads to a good behavior of the whole PV system.

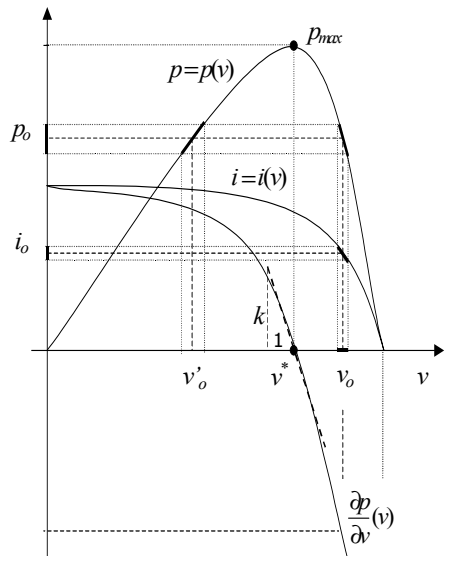

Fig. 2. Current, power, and power derivative of the PV panels vs. voltage

3. MPPT ALGORITHM ANALYSIS

All the MPPT algorithms are designed to dynamically extract the maximum power from the PV panels. Usually, the condition $\partial p/\partial v = 0$ is adopted to locate this operating point, since PV panels show a unique global maximum power point.

The MPPT algorithms are based on the determination of the slope of the PV panels output power versus voltage, i.e., the power derivative $\partial p/\partial v$. This quantity is utilized as representative of the "voltage error", i.e., the difference between the actual voltage of the PV panels and the reference voltage v^* corresponding to the maximum power operating point. The qualitative behavior of $\partial p/\partial v$ is represented in Fig. 2. In the region nearby v^* the power derivative can be considered a straight line having the slope k.

In order to determine the power derivative $\partial p/\partial v$ it is necessary to introduce a voltage and current perturbation around any operating point of the PV array. Traditional MPPT algorithms are based on "perturbation and observation" method or "incremental conductance" method. Some variants to these methods have been presented in order to improve the dynamic performance and/or to reduce undesired oscillations around the MPP (Kuo *et al*., 2001; Kim *et al*., 2001). An alternative method is based on measuring and processing the current and/or voltage ripple due to the switching behavior of the converter connected to the PV panels array. This method is known as "ripple correlation control", firstly proposed by Midya (1996) and successively utilized by Brambilla (1999) and Logue (2001). However, for small power PV generation systems, high switching frequency converters are usually adopted, reducing the residual voltage and

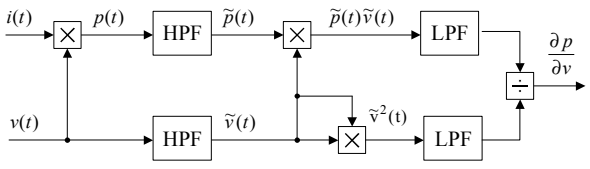

Fig. 3. Estimation of the PV power derivative by using filtering blocks.

current ripple below practical exploitable values.
In order to overcome this problems, in this paper a MPPT algorithm is proposed, which is based on the application of the "ripple correlation control", using the double-frequency oscillation of the instantaneous power as perturbation signals. The oscillations of the instantaneous power are inherent in a single-phase PV systems and can be considered itself as an embedded dynamic test signal useful to determine $\partial p/\partial v$. A key feature of this method is the knowledge of the oscillations period $T = 1/(2f)$ to improve the MPPT algorithm performances, being f the grid frequency.
The application of the "ripple correlation control", combined with the use of the $2f$ power oscillation, can be considered the main contribution of this paper for improving the performance of single-phase PV systems. The basic principle will be described with more detail in the following. For this purpose, let us consider a periodic function $x(t)$ having the moving average component $\bar{x}(t)$ over the period T, and the alternative component $\tilde{x}(t)$, respectively defined as

$$\bar{x}(t) = \frac{1}{T}\int_{t-T}^{t} x(\tau)d\tau, \tag{3}$$

$$\tilde{x}(t) = x(t) - \bar{x}(t). \tag{4}$$

Applying these definitions to the output voltage and power of the PV panels, leads to

$$v(t) = \bar{v}(t) + \tilde{v}(t), \quad p(t) = \bar{p}(t) + \tilde{p}(t). \tag{5}$$

The average operating point (v_o , p_o) on the $p = p(v)$ characteristic, and the corresponding voltage and power alternative components are represented in Fig. 2, according to the following expressions:

$$\bar{p}(t) = p(\bar{v}(t)) = p(v_o), \text{ being } v_o = \bar{v}(t). \tag{6}$$

Assuming the curve $p = p(v)$ still valid for dynamic analysis (Midya *et al.*, 1996) and linearizing nearby the average operating point $p_0 = p(v_0)$ leads to a relationship between the power ripple and the voltage ripple, expressed as

$$\tilde{p}(t) \cong \left(\frac{\partial p}{\partial v}\right)_{v_o} \tilde{v}(t). \tag{7}$$

The power derivative can be calculated by (7) as a function of power and voltage oscillations around the given operating point (v_o, p_o). In order to avoid critical calculations based on instantaneous power and voltage values, it is possible to introduce instead of (7) the moving average of the product of (7) and $\tilde{v}(t)$, leading to

$$\int_{t-T}^{t} \tilde{p}(\tau)\tilde{v}(\tau)d\tau \cong \left(\frac{\partial p}{\partial v}\right)_{v_o} \cdot \int_{t-T}^{t} \tilde{v}^2(\tau)d\tau. \tag{8}$$

Then, the power derivative can be evaluated as the following ratio:

$$\left(\frac{\partial p}{\partial v}\right)_{v_o} \cong \frac{\int_{t-T}^{t} \tilde{p}(\tau)\tilde{v}(\tau)d\tau}{\int_{t-T}^{t} \tilde{v}^2(\tau)d\tau}. \tag{9}$$

It can be noted that in (9) the power derivative is expressed in terms of integral quantities, and can be easy calculated. The voltage and power alternative components utilized in (10) can be evaluated on the basis of (3) and (4), leading to

$$\tilde{v}(t) = v(t) - \frac{1}{T}\int_{t-T}^{t} v(\tau)d\tau, \quad \tilde{p}(t) = p(t) - \frac{1}{T}\int_{t-T}^{t} p(\tau)d\tau. \tag{10}$$

Assuming the voltage and power oscillation frequency known, a filtering approach can be usefully adopted to extract the alternative components of $p(t)$ and $v(t)$. In particular, high-pass filters (HPF) can be used instead of (10). In the same way, low-pass filters (LPF) can be used instead of the moving averaging integrals of (9), as shown in the block diagram depicted in Fig. 3. Using this method it is possible to calculate the power derivative in a straightforward way, avoiding complicate and time consuming calculations.
The power derivative $\partial p/\partial v$ can be also used to represent the voltage error $\Delta v = v^* - v$, i.e., the difference between actual and MPP voltage, since the relationship between power and voltage is almost linear in the region around the MPP (see Fig. 2).

4. MPPT ALGORITHM IMPLEMENTATION

In order to implement the MPPT algorithm on a low cost DSP, without reducing its performance, the block diagram shown in Fig. 3 is further simplified. In particular, the average value of the product $\tilde{p} \cdot \tilde{v}$ could be conveniently utilized as the input variable of the dc-link voltage regulator. In fact, on the basis of (8), being the integral at the right-hand side always positive, the sign of the integral at the left-hand side corresponds to the sign of the power derivative $\partial p/\partial v$:

$$sign\left(\int_{t-T}^{t} \tilde{p}(t)\tilde{v}(t)dt\right) = sign\left(\frac{\partial p}{\partial v}\right). \tag{11}$$

The quantity $sign(\partial p/\partial v)$ is a clear indication of the region where the PV panel is working:

- $(\partial p/\partial v) > 0$ means $\tilde{p}$ and $\tilde{v}$ in phase agreement. The operating point is on the left side of the MPP on the *I-V* characteristic;
- $(\partial p/\partial v) < 0$ means $\tilde{p}$ and $\tilde{v}$ in phase opposition. The operating point is on the right side of the MPP on the *I-V* characteristic.

The knowledge of the instantaneous operating point region makes it possible to change the dc-link voltage reference in order to approach the maximum power

operating point. On the basis of these considerations, the scheme of Fig. 3 can be simplified leading to scheme represented in Fig. 4, where only the quantity corresponding to the average value of the product $\tilde{p} \cdot \tilde{v}$ and its sign are computed. In particular, the sign is extracted by a hysteretic comparator, set by a small band around zero, with the output values [-1,1] representing $sign(\partial p/\partial v)$.

5. DC-LINK VOLTAGE CONTROLLER

The scheme of the dc-link voltage controller is represented in Fig. 5. When $sign(\partial p/\partial v) > 0$ the integrator increases its output ΔV_{dc}, and the dc-link voltage reference V_{dc}^{*} moves towards the MPP. On the contrary, when $sign(\partial p/\partial v) < 0$ the integrator decreases ΔV_{dc} and the dc-link voltage reference V_{dc}^{*} moves back towards the MPP. The rate of change of V_{dc}^{*} is set by the gain K.

The input signal V_{dc}^{**} represents the initial voltage reference, i.e., the starting value of the integrator. When the control system is enabled, the quantity ΔV_{dc} computed by the MPPT algorithm is added to V_{dc}^{**}, giving the actual reference of the dc-link voltage V_{dc}^{*}. Then, the regulation of the current i_S injected into the mains allows the dc-link voltage to be controlled around the reference value. In this way, all the power coming from the PV generator is transferred to the grid. Following the reference value V_{dc}^{*} allows the PV panels to reach the maximum power operating point, where the condition $\partial p/\partial v = 0$ is satisfied.

The desired amplitude of the source current, I_S^{*}, is generated by the regulator $R(s)$, considering the dc-link voltage error $V_{dc} - V_{dc}^{*}$ as input variable. The reference value of the instantaneous source current i_S^{*} is generated on the basis of the amplitude I_S^{*}, and the phase angle of the fundamental component of the supply voltage v_S, which is represented by the unity sinusoid $\hat{v}_S^{1}$ in Fig. 5.

The measurement of the source current is used to implement the ac current control loop. The inverter is controlled on the basis of the instantaneous current error $\Delta i_S = i_S^{*} - i_S$, through a predictive PWM current regulator. In particular, the inverter reference voltage v_F^{*} is calculated by the voltage equation written across the ac-link inductance L_{ac}, according with the block diagram represented in Fig. 1. Neglecting the resistive effects and introducing a variational model, this equation yields

$$v_F^{*} = v_S + \frac{L_{ac}}{\Delta t}\Delta i_S \qquad (12)$$

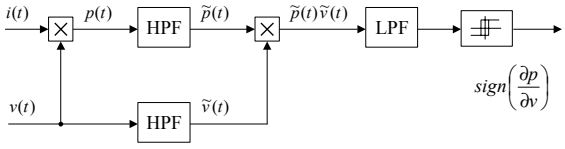

Fig. 4. Simplified estimation of the PV power derivative by using filtering blocks.

Table 1. Main characteristics of the pv generation system

Description	*Value*
Rated power of the PV system	P_{PV}=1.5 kW
Dc-link capacitance	C_{dc} = 2 mF
PWM carrier frequency	f_{sw} = 10 kHz
Ac-link inductor	R_{ac} = 0.1 Ω L_{ac} = 1 mH
Single phase utility grid	V_S=127 V f=50 Hz
Dc-link initial reference voltage	V_{dc}^{**} = 390 V
MPPT HPF: $\tau_{HPF}/(1+\tau_{HPF}s)$	τ_{HPF} = 0.05 s
MPPT LPF: $1/(1+\tau_{LPF}s)$	τ_{LPF} = 0.05 s
Dc-link voltage controller: PI type	K_P = 0.1 K_I = 10
Panels type (10 x, series connection)	Solar Shell SP150
Short circuit current (1 kW/m^2, 40 °C)	I_{sc} = 4.8 A
Open circuit voltage (1 kW/m^2, 40 °C)	V_{oc} = 420 V

The parameter $L_{ac}/\Delta t$ in (13) can be adjusted to obtain the desired regulator performance.

6. MPPT ALGORITHM VERIFICATION

The proposed MPPT algorithm has been verified by both numerical and experimental tests.

6.1 Simulation results

The numerical tests have been carried out by the Simulink environment of Matlab, with reference to a single-stage converter connected to a single-phase grid, as represented in Fig. 1. The PV panels have been electrically represented by the well-known single-exponential model , fitted on the I-V characteristic of a series array of ten modules Solar Shell SP150 type. The main characteristics of the PV generation system are summarized in Table I.

The main block diagrams of the implemented MPPT algorithm are summarized in Figs. 4 and 5.

The performance of the power conditioning system connected to the photovoltaic array has been evaluated both in steady state and transient operating conditions determined by start up and solar irradiance variations.

In Figs. 6-7 the behaviour of the control system in steady state conditions is represented. In particular, Fig. 6 shows the behaviour of $\tilde{v}$ and $\tilde{p}$ around the maximum power point. Initially, $\tilde{v}$ and $\tilde{p}$ are in phase agreement, i.e., the operating point of the PV modules is on the left side of the MPP on the *I-V* characteristic. Successively, $\tilde{v}$ and $\tilde{p}$ become in phase opposition, i.e., the operating point of the PV modules is on the right side of the MPP on the *I-V* curve. For all the operating conditions the frequency

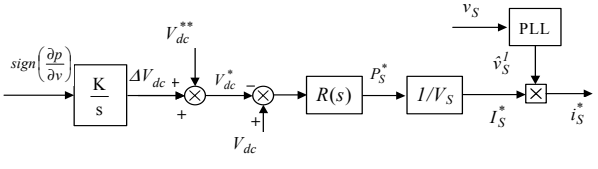

Fig. 5. dc-link voltage controller

of $\tilde{v}$ and $\tilde{p}$ is always twice than that of the grid.

In Fig. 7 the voltage and the grid current are represented in steady-state conditions. As expected, the current i_S injected into the grid is exactly in phase agreement with the grid voltage v_S.

6.2 Experimental results

The proposed control system for a single-phase, single-stage converter has been implemented on a laboratory prototype, where the PV panels have been replaced by an electric circuit, which behaves as a power generator having an output characteristic similar to that of the PV panels. The *P-V* characteristic of this electric source is given in Fig. 8. In this case the open circuit voltage is 500 V and the MPP is achieved with a dc-link voltage of 250 V. A better representation of the I-V characteristic of the photovoltaic panel is proposed by Grandi (2003), introducing a hardware model of the PV panels based on power electronic model. Fig. 9 shows the steady-state waveforms of voltage and current at the utility grid side. It can be noted that the resulting grid current i_S is sinusoidal and in phase agreement with the fundamental components of the grid voltage v_S, although the grid voltage has a low order harmonic distortion. Figs. 10 and 11 show the behaviour of the proposed MPPT algorithm during the start-up of the whole PV generation system. The initial output voltage of the power generator, when the converter is disabled, corresponds to the open circuit voltage (500 V).

When the system is enabled the reference dc-link voltage moves from the starting value (400 V) towards the maximum power point (250 V).

During the seeking of the MPP the dc-link voltage V_{dc} is always close to the reference voltage V_{dc}^* given by the MPPT algorithm. At the start-up, the dc-link voltage regulator guarantees the matching between the reference voltage V_{dc}^* and the dc-link voltage V_{dc} in about 0.2 s, then the MPP is reached in about 7 s.

Figs. 12 and 13 show the performance of the proposed MPPT algorithm in response to a step variation 25 A → 20 A of the short circuit current of the generator, corresponding to a 20% decrease of the solar irradiance. The operating point moves from ① to the new MPP in ② in 0.5s. Once the new MPP is reached, only small oscillations persist around the MPP.

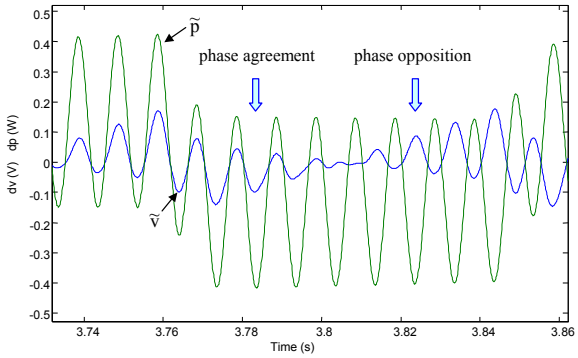

Fig. 6. Alternative components, $\tilde{v}$ and $\tilde{p}$.

7. CONCLUSION

A novel control strategy for single-stage converters connecting PV panels to a single-phase grid is proposed in this paper. The embedded MPPT algorithm is able to find the maximum power point by computing the sign of the PV power derivative versus voltage. This computation exploits PV current and voltage oscillations, at a frequency twice than that of the grid, due to the connection of the converter with a single-phase grid. The proposed MPPT algorithm does not require the knowledge of the model of the PV panels.

Once the power derivative has been computed by the MPPT algorithm, the dc-link voltage regulator drives the PV panels voltage toward the MPP value. The current regulator ensures steady state sinusoidal current and unity power factor also in presence of grid voltage perturbations.

The whole PV generation system has been numerically simulated and experimentally tested by a laboratory prototype. The results show good performance of the proposed control system in both steady-state and dynamic conditions, confirming the effectiveness of the PV generation for any operating condition.

REFERENCES

Brambilla A., Gambarara M., Garutti A., Ronchi F. (1999). "New approach to photovoltaic arrays maximum power point tracking", *Proc. of 30th Annual IEEE Power Electronics Specialists Conference*, PESC 1999, Vol. 2, pp. 632-637.

Gow J.A., Manning C.D. (2000). "Photovoltaic converter system suitable for use in small scale stand-alone or grid connected applications", *IEE Proceedings of Electric Power Applications*, Vol. 147, No. 6, pp. 535-543, Nov. 2000.

Grandi G., Sancineto G. (2003). "Hardware Modeling of Photovoltaic Panels", *Proc. of ISES Solar Congress*, Göteborg, (Sweden), June 14-19, 2003.

Kim T.Y., Ahn H.G., Park S.K., Lee Y.K. (2001). "A novel maximum power point tracking control for photovoltaic power system under rapidly changing solar radiation", *Proc. of IEEE-ISIE*, 2001, Pusan, Korea, Vol. 2, pp. 1011-1014.

Kuo Y.C., Liang T.J., Chen J.F. (2001). "Novel maximum-power-point-tracking controller for photovoltaic energy conversion system", *IEEE Trans. on Industrial Electronics*, Vol. 48 No. 3, pp. 594-601, June 2001.

Logue D.L., Krein P.T. (2001). "Optimization of power electronic systems using ripple correlation control: a dynamic programming approach", *Proc. of IEEE Power Electronics Specialists Conference*, PESC 2001, Vol. 2, pp. 459-464.

Midya P., Krein P.T., Turnbull R.J., Reppa R., Kimball J. (1996). "Dynamic maximum power point tracker for photovoltaic applications", *Proc. of 27th Annual IEEE Power Electronics Specialists Conference*, PESC 1996, Vol. 2, pp. 1710-1716.

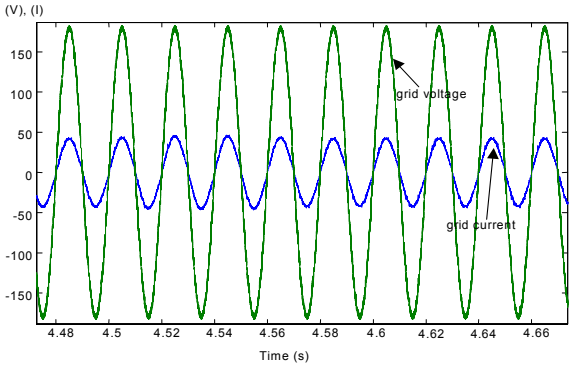

Fig. 7. Grid voltage and grid current at steady-state.

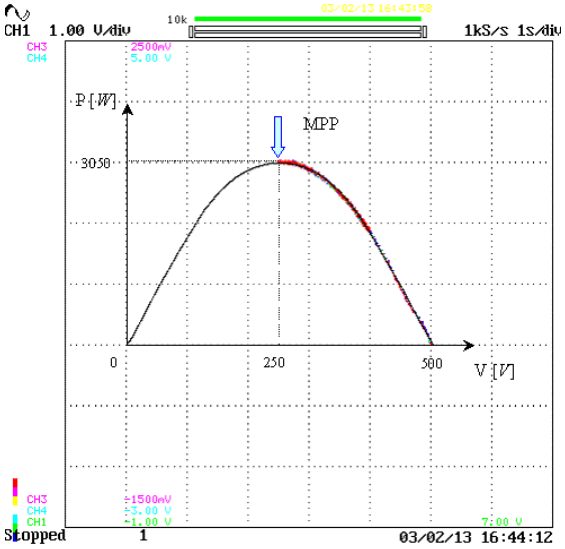

Fig. 8. *P-V* characteristic of the power generator replacing the PV panels.

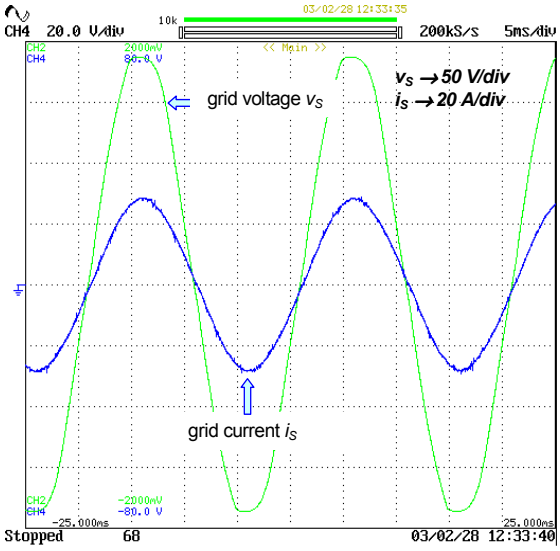

Fig. 9. Grid current i_S and grid voltage v_S in steady-state condition.

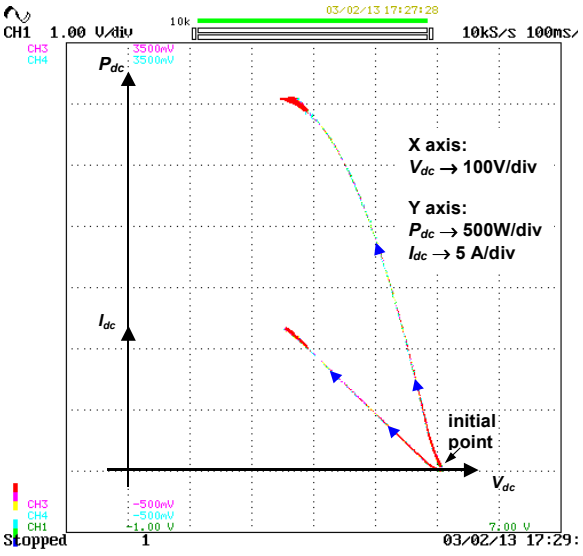

Fig. 10. *P-V* and *I-V* characteristic, representing the transient during the start-up of the PV generation system.

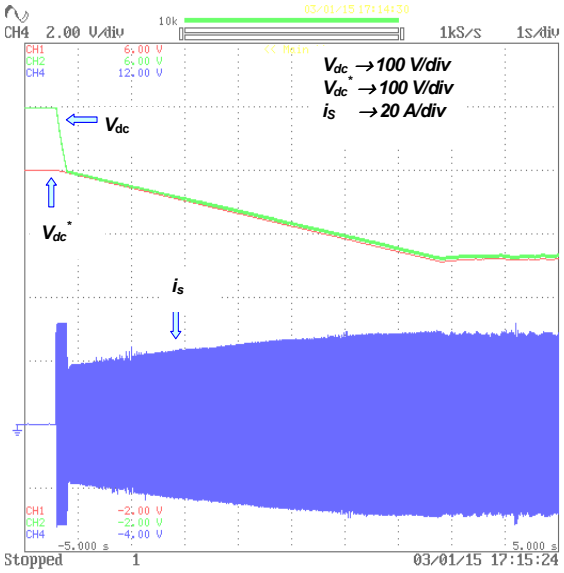

Fig. 11. V_{dc}^*, V_{dc}, and i_S during the start-up.

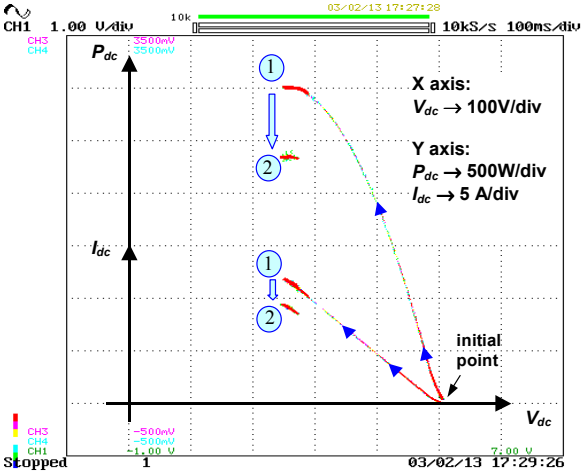

Fig. 12. *P-V* and *I-V* characteristic during a step change of the solar irradiance.

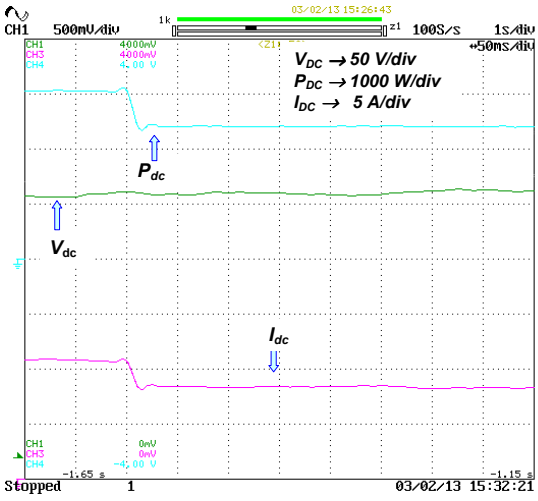

Fig. 13. Power, voltage and current supplied by the PV generation system vs. time during a transient representing a step change of the solar irradiance.